

The Quenching of the OH ($^2\Sigma^+$) Produced in the H_2 - O_2 Reaction by Collision with Ar

Yoshiaki HIDAHA,* Hiroyuki KAWANO, and Masao SUGA

Department of Chemistry, Faculty of Science, Ehime University, Bunkyo-cho, Matsuyama 790

(Received November 14, 1981)

Synopsis. H_2 - O_2 mixtures highly diluted with Ar were heated to temperatures in the range of 1200–1800 K behind reflected shock waves. The OH*-emission intensity was then measured to determine its quenching-rate constant upon collision with Ar; this constant was found to be about 1/164 of that in the case of H_2O .

The ultraviolet-band system OH ($^2\Sigma^+ - ^2\Pi$) is the most prominent feature in the emission spectra of flames sustained by the oxidation of hydrogenous compounds. A number of studies have been made to clarify the mechanism of OH* ($^2\Sigma^+$) formation in various systems. The collisional quenching of OH* has also been studied by several authors.^{1–6} It has been reported that the quenching effect of H_2O is considerably larger than those of other species, while that of Ar is very small. The quenching cross-sections (Q) of Ar reported are very scattered ($Q < 0.01 - Q < 2\text{\AA}^2$),^{1,6} even though scarcely cross-sections at high temperatures have been reported. In this report, we will describe OH* emission measurements in the H_2 - O_2 reaction, measurements undertaken in order to determine the quenching-rate constant by Ar.

Experimental

The apparatus and procedures are essentially the same as have been described previously.^{7–9} Emission was monitored with a Hamamatsu R-306 photomultiplier through an interference filter ($\lambda_{\text{max}} = 305.5\text{ nm}$, half-width = 15 nm) located behind a quartz window of the shock tube and through two slits with widths of 0.14 and 0.17 mm, separated by a cylindrical tube.

The computer calculation was carried out based on the Gear-type integration of the set of differential equations describing the chemical kinetics under constant-density conditions for reflected shock waves.

The compositions of the reaction mixtures were:

(A) 0.50% H_2 , 0.25% O_2 , 99.25% Ar,

(B) 1.00% H_2 , 1.00% O_2 , 98.00% Ar.

The H_2 , O_2 , and Ar, specified as 99.9%, 99.9%, and 99.99% pure respectively, were obtained from commercial cylinders and were used without further purification. The initial pressures of the mixtures were about 0.13 atm.

Results and Discussion

Two mixtures, (A) and (B), were heated to temperatures in the range of 1200–1800 K behind reflected shock waves. The typical OH* emission profiles observed with these two mixtures, (A) and (B), are shown in Fig. 1, which also shows the computed [OH*] profiles. Since one volt of the signal corresponds to $4.9 \times 10^{-15}\text{ mol cm}^{-3}$ of [OH*] under our experimental conditions,⁹ the observed OH* emission intensity can readily be converted into the OH* concentration. In Fig. 2, a plot of $\log I_B/I_A$ vs. T is shown, together with the simulation results, where I_A and I_B are the maximum OH* emission intensities measured with Mixtures (A) and (B) respectively.

The OH* formed in the H_2 - O_2 reaction may disappear by quenching:

OH* + M = OH + M,

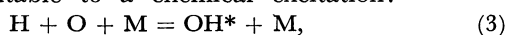


and by emission:



The reverse reaction (–1) is the thermal-excitation process, which contributes much less than the chemical excitation pathway at temperatures below 2000 K.¹¹ The reverse reaction (–2) is the self-absorption process, the extinction coefficient of which is small enough for to be disregarded.¹¹ Therefore, aside from quenching effects, the OH*-emission intensity observed below 2000 K may be assumed to be proportional to the chemiluminescent OH* concentration. For computations, the value of $k_2 = 1.4 \times 10^6\text{ s}^{-1}$ ¹² is used as the rate constant of Reaction (2).

Reaction (3) is adopted as the OH*-formation process attributable to a chemical excitation:⁹



whose rate constant is assumed to have the value of $k_3 = 1.2 \times 10^{13} \exp(-6940/RT)\text{ cm}^6\text{ mol}^{-2}\text{ s}^{-1}$.⁹ The maximum concentration ratios, $\alpha = [\text{OH}^*]_B/[\text{OH}^*]_A$, calculated for the two mixtures, (A) and (B), are independent of k_3 , which is changed by a factor of 10. The value of α is also independent of the mechanism of the OH*-formation reaction (bimolecular or termolecular reaction). Computations are performed by using a mechanism including:

- (a) 14 reactions and their rate constants for the H_2 - O_2 reaction reported by Olson and Gardiner,¹⁰ and

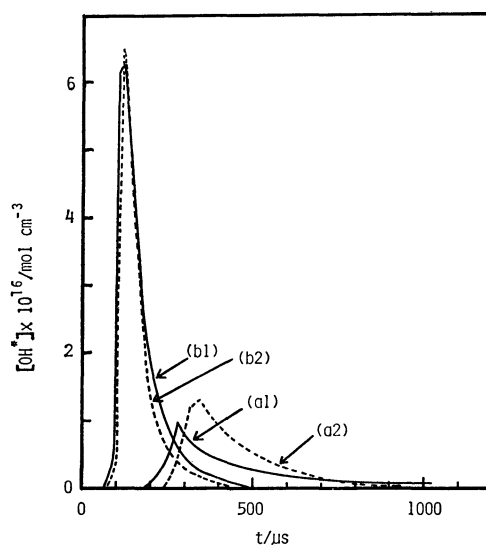


Fig. 1. Comparison of observed OH* emission profiles with [OH*] profiles computed by using $k_1(\text{M}=\text{Ar}) = 5.2 \times 10^{10} T^{0.5}$ and $k_1(\text{M}=\text{H}_2\text{O}) = 8.6 \times 10^{12} T^{0.5}$. Profile (a1): observed at 1400 K with Mixture (A), Profile (a2): computed at 1400 K for Mixture (A), Profile (b1): observed at 1358 K with Mixture (B), Profile (b2): computed at 1358 K for Mixture (B).

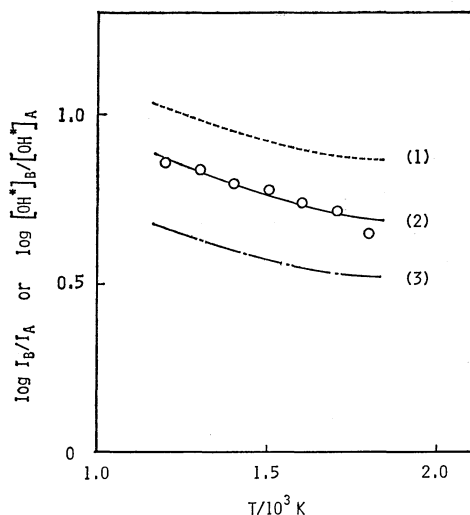


Fig. 2. Temperature dependence of the observed maximum OH* emission intensity ratio (open circle) and of the maximum OH* concentration ratio calculated for Mixtures (A) and (B).

Curve (1): $[\text{OH}^*]_{\text{B}}/[\text{OH}^*]_{\text{A}}$ calculated by using $k_1(\text{M}=\text{Ar})=4.2 \times 10^{11} T^{0.5}$. Curve (2): $[\text{OH}^*]_{\text{B}}/[\text{OH}^*]_{\text{A}}$ calculated by using $k_1(\text{M}=\text{Ar})=5.2 \times 10^{10} T^{0.5}$ and $k_1(\text{M}=\text{H}_2\text{O})=8.6 \times 10^{12} T^{0.5}$. Curve (3): $[\text{OH}^*]_{\text{B}}/[\text{OH}^*]_{\text{A}}$ calculated by using $k_1(\text{M}=\text{H}_2\text{O})=8.6 \times 10^{12} T^{0.5}$.

(b) 3 reactions (1)–(3) and their rate constants as described above.

In the present system, this relation holds: $I_{\text{B}}/I_{\text{A}} = [\text{OH}^*]_{\text{B}}/[\text{OH}^*]_{\text{A}}$, where I_{A} and I_{B} are the maximum OH*-emission intensities measured with Mixtures (A) and (B) respectively.

Fluorescence measurements (Reaction (1)) in the burnt gases in a lean acetylene-oxygen flame have revealed that the collision cross-sections for quenching by O_2 , H_2O , and Ar are 7, 35, and below 2 \AA^2 respectively.¹⁾ Of these cross-sections, it is concluded that $k_1(\text{M}=\text{H}_2\text{O})=8.6 \times 10^{12} T^{0.5}$, $k_1(\text{M}=\text{O}_2)=1.5 \times 10^{12} T^{0.5}$, and $k_1(\text{M}=\text{Ar})=4.2 \times 10^{11} T^{0.5} \text{ cm}^3 \text{ mol}^{-1} \text{ s}^{-1}$ as the rate constants of Reaction (1). Since species such as H_2 , O, OH, and H are also present in the reaction system, the quenching by them should also be taken into account. As $k_1(\text{M}=\text{H}_2)$ at room temperature, values in the range of 3.6×10^{12} – $7.6 \times 10^{13} \text{ cm}^3 \text{ mol}^{-1} \text{ s}^{-1}$ have been reviewed.¹³⁾ Since the quenching data against H, O, and OH as collision partners with OH* have not been reported, it is assumed that H_2 , OH, H-atoms, and O-atoms have the same quenching rate as O_2 . When we assume that $k_1(\text{M}=\text{Ar})=5.2 \times 10^{10} T^{0.5} \text{ cm}^3 \text{ mol}^{-1} \text{ s}^{-1}$, kinetic analysis under our experimental conditions shows that the Ar gas plays a dominant role for the OH* quenching, and that the quenching by O_2 , H_2 , OH, H, and O is negligible in comparison with those by H_2O and Ar (see Ref. 9). Hence, the quenching reactions by O_2 , H_2 , OH, H, and O were disregarded in the final computations. When M in Reaction (1) is assumed to be H_2O , the calculated value of α is always smaller than that observed. When M is Ar, on the other hand, the value of α is always larger than that observed, as may be seen in Fig. 2. By trial and error,

it has been found that a curve calculated assuming that $k_1(\text{M}=\text{H}_2\text{O})/k_1(\text{M}=\text{Ar})=164$ fits the experimental data best, as shown in Fig. 2. Consequently, the collision cross-section ratio, $Q(\text{H}_2\text{O})/Q(\text{Ar})$, is 140. When the quenching-rate constant of H_2O is assumed to be $8.6 \times 10^{12} T^{0.5} \text{ cm}^3 \text{ mol}^{-1} \text{ s}^{-1}$ ($Q=35 \text{ \AA}^2$),¹⁾ that by Ar is $5.2 \times 10^{10} T^{0.5} \text{ cm}^3 \text{ mol}^{-1} \text{ s}^{-1}$ ($Q=0.25 \text{ \AA}^2$). In Fig. 1, the typical emission profiles observed in the (A) and (B) mixtures are compared with the $[\text{OH}^*]$ profiles computed. The maxima of the calculated $[\text{OH}^*]$ are slightly larger than those observed in both mixtures, while the maxima computed for some runs were found to be slightly smaller than the observed ones. Consequently, the profiles calculated with the expression $k_1=5.2 \times 10^{10} T^{0.5}$ ($\text{M}=\text{Ar}$) are concluded to fit the experimental results best.

Carrington¹⁾ has reported that the quenching cross-section of Ar over the temperature range of 850–1500 K is less than 2 \AA^2 , which corresponds to $k_1(\text{M}=\text{Ar}) < 1.2 \times 10^{13} \text{ cm}^3 \text{ mol}^{-1} \text{ s}^{-1}$.¹³⁾ This upper-limit value is much larger than values at room temperature¹³⁾ and is consistent with our observation.

The quenching by inert monoatomic gases is generally accepted to be inefficient compared with that by bi- or triatomic gas molecules. If the smallest value recommended by Schofield¹³⁾ is assumed at room temperature, our observation of the larger value at high temperatures must lead to the conclusion that $k_1(\text{M}=\text{Ar})$ is strongly dependent on the temperature. Assuming that a large kinetic energy of $\text{OH}^* + \text{Ar}$ collision is required to reach a crossing point of the potential curves of $\text{OH}^* + \text{Ar}$ and $\text{OH} + \text{Ar}$, $k_1(\text{M}=\text{Ar})$ increases at a higher temperature. However, no significant temperature-dependence of k_1 could be found under our temperature conditions (1200–1800 K). Such independence of $k_1(\text{M}=\text{Ar})$ conflicts with the quenching mechanism described above. In order to solve this difficulty, an experiment for the reliable determination of $k_1(\text{M}=\text{Ar})$ is desired over a wide temperature range from room temperature to several thousand K.

References

- 1) T. Carrington, *J. Chem. Phys.*, **30**, 1087 (1959).
- 2) V. N. Kondrat'ev, "Chemical Kinetics of Gas Reactions," Pergamon Press, New York (1964).
- 3) R. G. Bennett and F. W. Dalby, *J. Chem. Phys.*, **40**, 1414 (1964).
- 4) H. P. Hooyamers and C. Th. J. Alkemade, *J. Quant. Spectry. Radiative Transfer*, **7**, 495 (1967).
- 5) M. Kaneko, Y. Mori, and I. Tanaka, *J. Chem. Phys.*, **48**, 4468 (1968).
- 6) D. Kley and K. H. Welge, *J. Chem. Phys.*, **49**, 2870 (1968).
- 7) Y. Hidaka, T. Kataoka, and M. Suga, *Bull. Chem. Soc. Jpn.*, **47**, 2166 (1974).
- 8) Y. Hidaka, T. Nishi, and M. Suga, *Bull. Chem. Soc. Jpn.*, **49**, 2007 (1976).
- 9) Y. Hidaka, S. Takahashi, H. Kawano, M. Suga, and W. C. Gardiner, Jr., *J. Phys. Chem.*, **86**, 1429 (1982).
- 10) D. B. Olson and W. C. Gardiner, Jr., *Combust. Flame*, **32**, 151 (1978).
- 11) W. C. Gardiner, Jr., K. Morinaga, D. L. Ripley, and T. Takeyama, *Phys. Fluids Supplement*, **1**, 120 (1969).
- 12) K. R. German, *J. Chem. Phys.*, **62**, 2584 (1975).
- 13) K. Schofield, *J. Phys. Chem. Ref. Data*, **8**, 723 (1979).